CO Homologues Hot Paper

International Edition: DOI: 10.1002/anie.201504863
German Edition: DOI: 10.1002/ange.201504863

{μ-PbSe}: A Heavy CO Homologue as an Unexpected Ligand

*Günther Thiele, Yannick Franzke, Florian Weigend, and Stefanie Dehnen**

Dedicated to Professor Manfred Scheer on the occasion of his 60th birthday

Abstract: *Reactions of $[K(18\text{-crown-}6)]_2[Pb_2Se_3]$ and $[K([2.2.2]crypt)]_2[Pb_2Se_3]$ with $[Rh(PPh_3)_3Cl]$ in en (ethane-1,2-diamine) afforded ionic compounds with $[Rh_3(PPh_3)_6(\mu_3\text{-}Se)_2]^-$ and $[Rh_3(CN)_2(PPh_3)_4(\mu_3\text{-}Se)_2(\mu\text{-}PbSe)]^{3-}$ anions, respectively. The latter contains a PbSe ligand, a rather uncommon homologue of CO that acts as a μ-bridge between two Rh atoms. Quantum chemical calculations yield a significantly higher bond energy for PbSe than for CO, since the size of the ligand orbitals better matches the comparably rigid Rh-Se-Rh angles and the resulting Rh···Rh distance. To rationalize the bent coordination of the ligand, orbitals with significant ligand contributions and their dependence on the bonding angle were investigated in detail.*

The importance of CO, both as a ligand and a reactant, can hardly be overestimated. The publication of a total of 43 reviews in *Angewandte Chemie*, 41 in *Chemical Reviews*, and more than 50 in *Coordination Chemistry Reviews* within the last decade reflects the huge diversity of syntheses and catalytic applications of carbon monoxide and its compounds.

In contrast, apart from matrix isolation experiments,[1] the molecular and coordination chemistry of the heavier homologues of CO, thus the neutral molecular tetrel monochalcogenides $E^{14}E^{16}$ (E^{14} = C…Pb; E^{16} = O…Te), with (formally) divalent E^{14}(II) atoms, is restricted to complexes with carbon monochalcogenides CS, CSe, and CTe.[2a] Furthermore, SnO and PbO units were stabilized within pincer complexes using benzannulated bisstannylene ligands.[2b] All other examples were only discussed as intermediates in the context of spectroscopic[3–6] and/or theoretical studies,[4–16] such as molecular PbO which was obtained under single-atom-collision conditions from atomic Pb and O_3.[17]

The reason for the apparent difference between the chemistry of CO and that of its heavier homologues has been attributed to the distinctly lower bond strength of the corresponding "triple" bond with increasing atomic number, and therefore a higher tendency towards aggregation – ultimately yielding the respective minerals, such as litharge and massicot in the case of PbO.[18] Nevertheless, according to calculations on PbO and PbS minerals, the nature and role of the lone pair at the Pb atom is strongly influenced by the corresponding chalcogenide ion, ranging from only small contributions of the 6s atomic orbital (due to the mixing of states) in PbO to a rather high 6s contribution in the frontier orbital region of PbS.[19] Following this trend, a higher electron density on the tetrel atom is expected for the heavier homologues of the PbE^{16} series. Thus with E^{16} = Se or Te, ligand activity might become possible, which will be discussed herein.

In the synthesis of the mixed-valence compound $[(RhPPh_3)_6(\mu_3\text{-}Se)_8]\cdot 0.5\,en$[20] from solutions of $[K(18\text{-crown-}6)]_2[Pb_2Se_3]$[21] and $[Rh(PPh_3)_3Cl]$[22] in *en* (ethane-1,2-diamine), we detected small amounts of $\{[K(18\text{-crown-}6)][K(en)_2]K[Rh_3(CN)_2(PPh_3)_4(\mu_3\text{-}Se)_2(\mu\text{-}PbSe)]\}_2\cdot 1.3\,en$ (**1**, Figure 1), as a well-reproducible side-product.

The anion in **1** (Figure 1, top) is based on a $[Rh_3Se_2]$ trigonal bipyramid, with two μ_3-Se bridges (Se1, Se2) in axial and three Rh atoms (Rh1–Rh3) in equatorial positions. At first glance, the Rh atoms adopt an approximately square-planar coordination through two Se atoms (cis) and two further ligands: two PPh_3 groups at Rh1, and one PPh_3 and one CN^- ligand at Rh2 and Rh3. However, the bonding environment of the latter is extended towards a (distorted) square pyramid by a μ-bridging Pb atom (Pb1) that is bonded to an Se atom (Se3). Pb1, in turn, forms three bonds (Pb1–Rh2, Pb1–Rh3, and Pb-1-Se3) in a trigonal-pyramidal manner, which is in accordance with the expectation for a formal Pb^{II} atom.

Two clusters are interconnected by a total of six K^+ ions around an inversion center of the unit cell (Figure 1, bottom). While Se1 does not show significant interactions with the K^+ counterions, and Se2 has only one notable Se···K^+ contact (3.2331(9) Å), Se3 coordinates to five K^+ ions, thus adopting a near-octahedral μ_6-bridging mode in the sum. One of the K^+ ions (K2) is additionally coordinated by a 18-crown-6 molecule; the others show a multiple ligand situation including one further O atom per crown ether molecule, both N

[*] Dr. G. Thiele, Prof. Dr. S. Dehnen
Fachbereich Chemie und Wissenschaftliches Zentrum
für Materialwissenschaften, Philipps-Universität Marburg
Hans-Meerwein-Strasse 4, 35032 Marburg (Germany)
E-mail: dehnen@chemie.uni-marburg.de
Y. Franzke, Priv.-Doz. Dr. F. Weigend
Institut für Physikalische Chemie
Karlsruher Institut für Technologie (KIT)
Fritz-Haber-Weg 2, 76131 Karlsruhe (Germany)
Priv.-Doz. Dr. F. Weigend
Institut für Nanotechnologie
Karlsruher Institut für Technologie
Hermann-von-Helmholtz Platz 1
76344 Eggenstein-Leopoldshafen (Germany)

Supporting information for this article is available on the WWW under http://dx.doi.org/10.1002/anie.201504863.

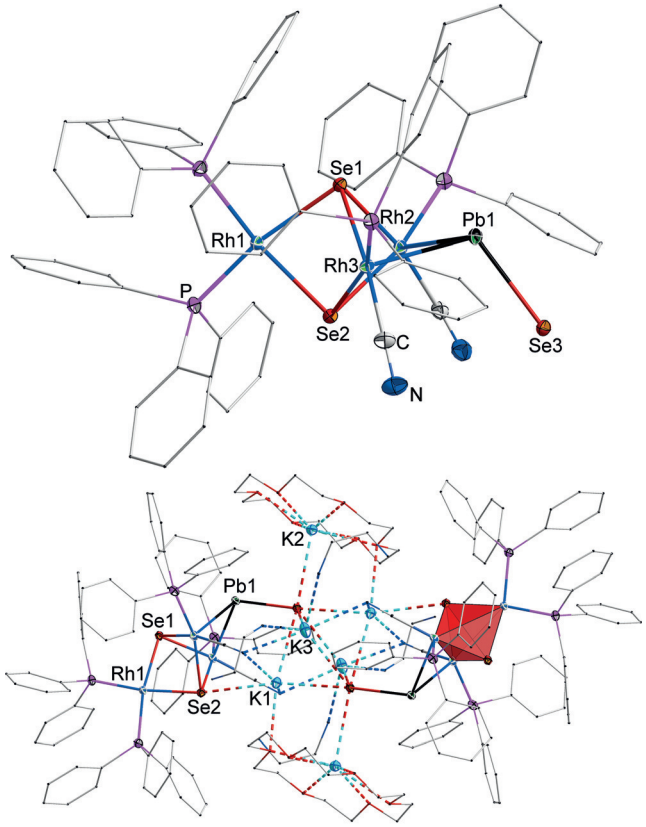

Figure 1. Top: Molecular structure of the anion in **1**. Ellipsoids are drawn at 50% probability. Disorder of Se3 (see Figure S4) and H atoms are omitted for clarity. Phenyl groups are drawn as wires. Selected structural parameters [Å/°]: Rh–Se 2.4563(4)–2.4868(5), Rh–Pb 2.7542(3)–2.7576(3), Pb–Se 2.647(4) and 2.7105(6) (disorder), Rh(2,3)···Rh1 3.3217(7)–3.4982(6), Rh2···Rh3 2.9604(4), K···Se2 3.2331(9) Å, K···Se3 3.165(5)–3.593(2); Rh–Pb–Rh 64.972(9), Se–Pb–Rh 106.54(10)–119-09(8), Se–Rh–Pb 83.691(12)–83.773(12) and 103.701(13)–103.959(13), Se–Rh–Se 79.333(14)–80.273(14), Pb–Rh–P 92.34(3)–94.06(3). Bottom: Dimeric unit in **1** with one $[Rh_3Se_2]$ polyhedron highlighted. Organic groups are drawn as wires. Noncoordinating solvent molecules and disorder omitted for clarity.

atoms of the CN^- ligands, and N atoms from solvent *en* molecules besides one (K2, K3) or two (K1) Se neighbors.

The list of crystallographically determined compounds that contain bonding Pb–Se interactions of any kind can be classified into three groups: a) inorganic solid-state phases, ranging from binary PbSe (clausthalite[23] besides two high-pressure modifications[24]) and $Pb(Se_2)$[25] to multinary phases such as $Cd(In_{0.4}Bi_{0.6})PbBi_3(Se_{0.05}S_{0.95})_8$;[26] b) (element-) organic compounds without any further Pb–M or Se–M bonds ($M \neq Pb$), such as $Ph_3Pb(\mu\text{-}Se)P(OEt)_2Se$[27] and $(AsPh_4)[Pb(SePh)_3]$;[28] and c) a total of three complexes with further Se–M (but no Pb–M) bonds, namely $[(Pt(PPh_3)_2)_2(PbSe_2)]NO_3\cdot CH_2Cl_2$,[29] $(PPh_4)_4[Pb_2W_4Se_{16}]$,[30] and $[Eu\{Pb(SePh)_3\}(thf)]$.[31] In the latter three cases, coordination to further metal ions is always achieved via Se ligands, and Pb ions are bound to at least two Se atoms. Thus, apart from **1**, none of the compounds known to date contain a PbSe fragment with coordination behavior reminiscent of that of CO, in other words coordination through the Pb atom. Further, to the best of our knowledge, no molecular compound with an Rh–Pb bond has yet been isolated or properly characterized. The only indication for the formation of such a species was obtained by tentative IR and mass spectra of a reaction mixture that apparently contained the Rh^I complex $[CpRh(CO)(PbMe_3)_2]$, possessing terminal trimethylplumbyl ligands.[32]

The CN^- ions are likely a result of C–C bond cleavage and dehydration of the solvent *en*, the only C/N source in the reaction solution. We have observed the decomposition of *en* in the presence of a K/Pb/Se species previously,[33a] however, with formation of NH_3. Thus the formation of CN^- might be mediated (or possible catalyzed) by the $[Rh(PPh_3)_3Cl]$ complex here [see Eq. (1)]. Intentional addition of KCN to the reaction solution increases the reaction yield of single crystals of **1** by a factor of three.

$$H_2N\text{-}CH_2\text{-}CH_2\text{-}NH_2 \xrightarrow{(Rh)} 2\,CN^- + 2\,H^+ + 3\,H_2 \qquad (1)$$

Further attempts to increase the yield by variation of the solvent only afforded solvent pseudo polymorphs of **1**,[33b] while the replacement of 18-crown-6 with [2.2.2]crypt by utilization of $[K([2.2.2]crypt)]_2[Pb_2Se_3]$[34] as the starting material leads to the formation of $[K([2.2.2]crypt)[Rh_3(PPh_3)_6(\mu_3\text{-}Se)_2]\cdot 3\,C_6H_6$ (**2**). The latter is also based on an $[Rh_3Se_2]$ trigonal bipyramid, but unlike the situation in **1**, all Rh atoms exhibit an approximately square-planar coordination through two Se atoms and two PPh_3 ligands (Figure 2).

To further investigate the properties of the highly unusual and unexpected PbSe ligand, its similarities to and differences from the CO homologue and its μ-bridging interaction with the Rh/Se cluster, comprehensive quantum chemical calculations were performed. The calculations served to answer the following questions: 1) Can the anion in **1** form from that in **2** and what are the energetics for a hypothetical CO-bridged homologue? 2) What are the differences between molecular

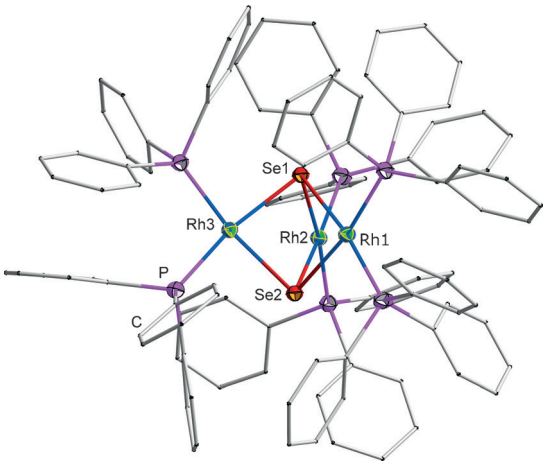

Figure 2. Molecular structure of the $\{[(Ph_3P)_2Rh]_3(\mu_3\text{-}Se)_2\}^-$ anion in **2**. Ellipsoids are drawn at 50% probability, H atoms are omitted, phenyl groups are drawn as wires. Selected structural parameters [Å/°]: Rh–P 2.2307(7)–2.2372(7), Rh–Se 2.4619(3)–2.4701(3), Rh···Rh 3.2263(9)–3.3534(5); Se–Rh–Se 79.493(10)–79.598(10), Rh–Se–Rh 81.802(10)–85.775(10), P–Rh–P 98.89(3)–101.18(3), P–Rh–Se 88.76(2)–91.743(19).

PbSe and CO and how does this affect the bonding in the anion in **1** and the hypothetical CO homologue?

To answer the first question, structure parameters were optimized at the TPSS/dhf-TZVP level (see the Computational Methods in the Experimental Section) for the anions in **1** and **2** as well as for all further reactants along a formal reaction pathway from the latter to the former, i.e., PPh_3, $(CN)^-$, and PbSe. For comparison, the CO homologue of the anion in **1** and CO itself were calculated by the same methods. Scheme 1 summarizes the results.

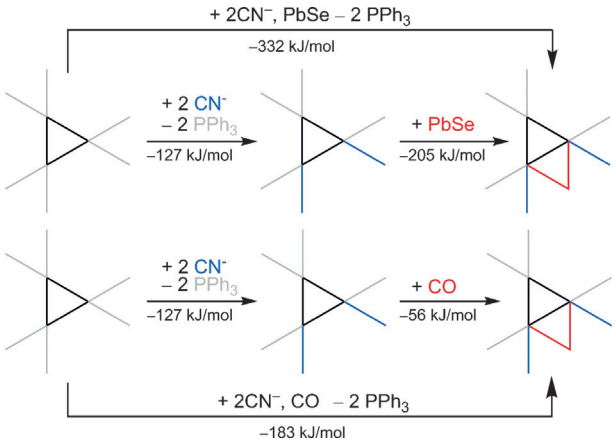

Scheme 1. Calculated reaction pathway from the anion in **2** (left-hand side) to the anion in **1** (top right), or to a hypothetical CO homologue (bottom right). Black triangles represent the $[Rh_3Se_2]$ unit, gray terminal lines denote PPh_3 ligands, blue terminal lines denote $(CN)^-$ ligands, red lines represent attachment of PbSe or CO.

The formation of the anion in **1** from the anion in **2** is exoenergetic by ca. 330 kJ mol^{-1}; the corresponding reaction of the CO analogue is also exoenergetic, but only by ca. 180 kJ mol^{-1}, because the bond energy for the CO unit in the cluster (56 kJ mol^{-1}) is much lower than that for the PbSe unit (205 kJ mol^{-1}). The reasons for these differences were investigated as detailed in the following, starting with the analysis of the local geometry of the coordination mode (Table 1).

The angle ϕ formed between the Pb–Se bond and the Rh-Pb-Rh plane was calculated to 59.3° (experimental: 59.4°), and the calculated (nonbonding) distance of the two Rh atoms bridged by PbSe is 3.058 Å (experimental: 2.960 Å), which is 0.313 Å shorter than in the unbridged case. CO in contrast coordinates to the cluster in an (almost) planar fashion, the corresponding angle ϕ amounts to 3.3°. Further, the Rh···Rh distance (2.681 Å) is much smaller than that calculated for the PbSe-bridged system; of course, it is again much smaller than that without bridging, but distinctly longer than reported recently for a CO-μ-bridged Rh–Rh bond (2.437 Å).[35]

To investigate the reasons for the differences between CO and PbSe in terms of bond energy and coordination, we considered a simpler model. Phenyl ligands were replaced with hydrogen. In this way, C_s symmetry could be used and thus the MOs perpendicular to the mirror plane and MOs within this plane could be distinguished, which was helpful for the discussion below. Energies and structure parameters, in particular those of the bent coordination, are well reproduced this way (see Table 1). This is also true for the BP86/SV(P) method, which is used in the following.

The comparably low bond energy for a hypothetical μ-bridging by CO is accompanied by significant changes in the structure parameters relative to the unbridged cluster, mainly reflected by the change in the Rh···Rh distance (in the simplified model: 3.288 Å for the unbridged system, 3.049 Å with PbSe, and 2.727 Å with CO as a bridge, respectively, see Table 1). This is because C has a significantly smaller atomic size than Pb, causing a structural strain, which is identified as the main reason for disfavoring CO. It can be quantified by first calculating the energy of the entire system (with optimized structure parameters, line "BE" in Table 1) and that of the fragments without further optimization (line "BE_{unr}" in Table 1). Next, the energetic effect of the distortion in the cluster (plus that in the ligand) is obtained from the corresponding difference $BE_{unr}-BE$, denoted as relaxation energy "RE" in Table 1. Since similar BE_{unr} values are obtained for both PbSe and CO (175 kJ mol^{-1} and 204 kJ mol^{-1}, respectively) RE amounts to only 30 kJ mol^{-1} for the PbSe-bridged cluster, but to ca. 170 kJ mol^{-1} for the CO-bridged analogue, which finally confirms the mismatch of CO as a bridging ligand here.

It remains to clarify the differences in the coordination mode, reflected by the angle ϕ. The MOs of isolated CO and PbSe are presented in Figure 3, illustrating an inverse order of σ_{pz} and π MOs (HOMO−1 and HOMO, respectively) in PbSe

Table 1: Calculated structure parameters and bond energies for anions $[Rh_3(CN)_2(PPh_3)_4(\mu_3\text{-}Se)_2(\mu\text{-}L)]^{3-}$ with L = PbSe or CO at level TPSS/dhf-TZVP, denoted "full", and for the simplified C_s symmetric model $[Rh_3(CN)_2(PH_3)_4(\mu_3\text{-}Se)_2(\mu\text{-}L)]^{3-}$ at the same level as well as at level BP86/dhf-SV(P).[a]

Level	Expt.	Full TPSS/dhf-TZVP		Simplified TPSS/dhf-TZVP		Simplified BP86/dhf-SV(P)	
L	PbSe	PbSe	CO	PbSe	CO	PbSe	CO
$d_{Pb/C-Se/O}$ [Å]	2.719	2.699	1.200	2.642	1.197	2.635	1.205
$d_{Pb/C-Rh}$ [Å]	2.804, 2.798	2.797, 2.788	2.053, 2.033	2.861	2.058	2.888	2.045
$d_{Rh\cdots Rh}$ [Å]	2.960	3.058	2.681	3.039	2.680	3.049	2.727
ϕ [°]	59.4	59.3	3.3	61.0	0.7	57.8	1.3
BE [kJ mol^{-1}]	–	205	56	164	39	145	36
BE_{unr} [kJ mol^{-1}]	–	–	–	180	203	175	204
RE [kJ mol^{-1}]	–	–	–	16	164	30	168

[a] ϕ denotes the angle of the Pb–Se/C–O bond with the Rh–Pb/C-Rh plane. The bond energy BE refers to fully optimized systems, BE_{unr} is the energy difference of the structure-optimized entire system and the fragments without further structure optimization. The energetic effect of the cluster plus ligand distortion upon bond formation is reflected by the difference $BE_{unr}-BE = RE$ ("relaxation energy").

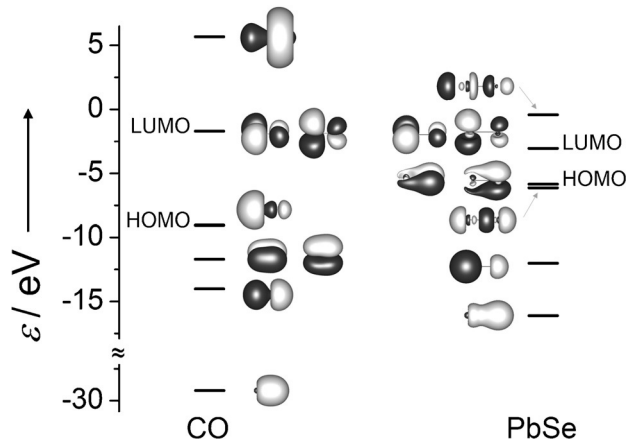

Figure 3. MO scheme of the frontier MOs of CO (left) and PbSe (right).

as compared to those in CO, a significantly smaller energy difference between the named MOs in PbSe, and different atomic contributions to them in the two homologue cases.

Next, MOs with significant contributions from the bridging ligand were identified by projection of the converged orbitals on the (orthogonalized) orbitals of the noninteracting fragments (see the Computational Methods); for these MOs also Mulliken overlap populations between C or Pb and Rh were calculated. This was done for the favored coordination modes, $\phi(CO) = 0°$ and $\phi(PbSe) = 58°$, as well as for "interchanged" modes with $\phi(CO) = 50°$ and $\phi(PbSe) = 0°$, which are higher in energy than the favored modes by 74 kJ mol^{-1} (CO) and 50 kJ mol^{-1} (PbSe), respectively. All orbitals with significant bridging ligand contributions (σ vs. π, donor-type vs. acceptor-type) are listed in the Supporting Information together with the corresponding contributions (Figures S10–S13 and Tables S4–S7). Most relevant for the issue discussed here are the orbitals that are most significantly affected by changes in ϕ. They are presented in Figure 4.

In the case of CO coordinated in a planar manner (upper left part of Figure 4), HOMO−10 (MO 107, orbital energy −4.8 eV, ca. 2 eV below the HOMO level) represents π back-donation. For this orbital, a contribution of 18% from the antibonding orbital of CO in the plane spanned by the C atom and the two Rh atoms, π_p^*, is observed. The HOMO is mainly localized on the cluster and is Rh–E^{14} antibonding (E^{14} = C), reflected by a comparably large negative value for the Mulliken overlap population of −0.161. For PbSe coordinated in a planar manner (lower left part of Figure 4), the corresponding orbital HOMO−3 (MO 135, orbital energy −4.0 eV, ca. 1 eV below the HOMO level) is essentially nonbonding; the Pb–Rh Mulliken overlap population of this MO is negligible. Moreover, the HOMO shows overall higher ligand contributions (mainly from Se) but is also Rh–E^{14} antibonding (E^{14} = Pb). None of the orbitals discussed so far were found to have significant contributions from the ligands' π_o^* orbital, which is orthogonal to the plane spanned by E^{14}, Rh2, and Rh3 (see Figure 1).

For the bent coordination, HOMO−10 (CO) and HOMO−3 (PbSe) are *de*stabilized compared to the planar coordination in both cases. Whereas the effect is large for CO (0.4 eV), it is small for PbSe (0.1 eV) since—like for the planar mode—the Pb–Rh Mulliken overlap population of this MO is negligible. The HOMO is stabilized in both cases due to a contribution from π_o^*, which weakens the antibonding character. For PbSe, this amounts to 28%, which leads to a stabilization by 0.4 eV relative to the planar case (−3.4 eV versus −3.0 eV) and to a reduction of the (negative) Mulliken overlap population by a factor of 3. The corresponding contribution in the case of CO is only 4%, resulting in a stabilization of only 0.2 eV (−2.9 eV versus −2.7 eV), and the Mulliken overlap population is reduced only by a factor of 1.6. These differences might come from the energetically less favorable accessibility of the π* orbitals of CO. If one adds, as a crude approximation, the effects of stabilization for the HOMO and destabilization for the non-HOMO, one gets 0.3 eV (ca. 30 kJ mol^{-1}) in favor of the bent coordination for PbSe and 0.2 eV (ca. 20 kJ mol^{-1}) in favor of the planar coordination in case of CO. This is (qualitatively) in line with the numbers resulting from total energies, 50 and 74 kJ mol^{-1} (see above).

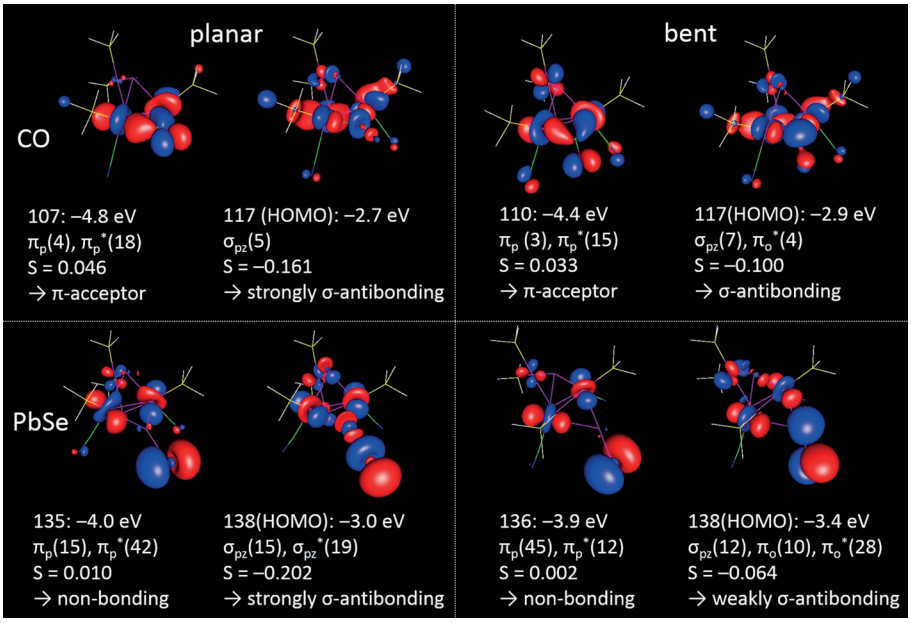

Figure 4. Orbitals most significantly affected by changes in ϕ, for CO (top) and PbSe (bottom) in planar (left) and bent (right) coordination for the model system. For each MO, the first number in the first line labels the MO, the second number gives its energy (in eV). In the second line, the contributions from the ligand orbitals are given in %, the third line displays the Mulliken overlap population, and the fourth line gives a summarizing characterization. For details see text.

So, the experimentally observed bent coordination of PbSe is mainly due to the admixture of π_o* to the HOMO of the entire cluster anion and the comparably small loss of bonding interaction as the relevant MO (CO: MO 107, PbSe: MO 135) is essentially nonbonding in the case of the heavier homologue. Additionally, the overall favoring of PbSe over CO as a ligand results from the better match of the Rh···Rh distance with the spatial extent of the orbitals of PbSe.

The situation is reminiscent of the *trans* bent arrangement of organic ligands R in $R_nE{=}ER_n$ units of "heavy" main-group elements E (that is, elements of period 3 and higher),[36] hence extending such systems by the rather uncommon replacement of the ligands R by the two adjacent Rh atoms of the cluster in **1**. However, as noted above, the combination $R_2E^{14}{=}E^{16}$ is rare for heavy elements anyway, with no precedence for E^{14}= Pb and E^{16}=Se so far.

Experimental Section

General: All manipulations and reactions were performed under an Ar atmosphere using standard Schlenk or glove box techniques. All manipulations with Pb species were performed under exclusion of light. Solutions of $[K(18\text{-crown-6})]_2[Pb_2Se_3]$ and $[K([2.2.2]crypt)]_2[Pb_2Se_3]$ were prepared according to literature procedures.[21] THF, toluene, and benzene were freshly distilled from NaK alloys prior use. $[Rh(PPh_3)_3Cl]$ (Sigma Aldrich) was dried under dynamic vacuum ($p < 1\times10^{-4}$ mbar) for at least 12 h. All starting materials were double-checked and proved to be cyanide-free.

Syntheses: **1**: A 10 mL portion of a saturated *en* solution of $[K(18\text{-crown-6})]_2[Pb_2Se_3]$ was carefully layered with 10 mL of a saturated THF solution of $[Rh(PPh_3)_3Cl]$. After 4 weeks, **1** crystallizes reproducibly along with $[Rh_6Se_8(PPh_3)_6]\cdot0.5\,en$[20] as a few black blocks per batch. The yield can be tripled upon addition of 20 mg of KCN. **2**: A 10 mL portion of an *en* solution of $[K([2.2.2]crypt)]_2[Pb_2Se_3]$ was carefully layered with 10 mL of a saturated THF solution of $[Rh(PPh_3)_3Cl]$. Compound **2** crystallizes after one week as brown blocks in approximately 25% yield. Energy-dispersive X-ray (EDX) spectroscopy served to confirm the heavy-element composition of compounds **1** and **2** (see the Supporting Information). However, the extremely low yield of compound **1** and intrinsic product mixtures in both cases inhibited further analyses.

Single-crystal X-ray diffraction: Data collection was performed using a Bruker Quest (**1**) or Stoe IPDS2T (**2**) diffractometer at 100 K with $Mo_{K\alpha}$ radiation and graphite monochromatization ($\lambda = 0.71073$). Structure solution was realized by direct methods, refinement with full-matrix least-squares against F^2 using SHELXS-97, SHELXL 2014, and Olex2 software.[37,38] Crystal data for $C_{182.67}H_{180}K_6N_{14.67}O_{12}P_8Pb_2Rh_6Se_6$ (**1**, $M_W = 4761.42\ g\,mol^{-1}$): $a = 17.4936(5)$, $b = 24.6283(7)$, $c = 22.2850(5)$ Å, $\beta = 91.7940(10)°$; $C_{144}H_{136}KN_2O_6P_6Rh_3Se_2$ (**2**, $M_W = 2682.11\ g\,mol^{-1}$): $a = 15.7285(4)$, $b = 33.0820(7)$, $c = 24.6448(7)$ Å, $\beta = 106.220(2)°$. CCDC 1402659 (**1**) and 1402660 (**2**) contain the supplementary crystallographic data for this paper. These data can be obtained free of charge from The Cambridge Crystallographic Data Centre.

Computational methods: Calculations were done with the program system TURBOMOLE;[39,40] the RI approximation[41] and the conductor-like screening model (COSMO)[42] were applied throughout, the latter with default settings except for the radii, which were increased by 10% in order to improve convergence of the structure optimization procedure. For the calculations of the anion in **1** the TPSS[43] functional was chosen with basis sets of polarized triple zeta valence quality, dhf-TZVP,[44] together with corresponding effective core potentials for Rh[45] and Pb.[46] For the calculations of the model system dhf-SV(P)[44] bases and the BP86[47,48] functional were used. The contributions of the valence orbitals of CO/PbSe ligand to the MOs of the entire system were computed as follows. First, the system was decomposed into bare cluster and CO/PbSe ligand. The MOs of the subunits were calculated separately. After convergence, the product wave function for the entire system was constructed from these MOs and orthogonalized (like in the energy decomposition analysis[49] procedure), yielding the MOs $\phi_p{}^0$. Their contributions to the converged MOs ϕ_q (Figure 4) are the scalar products $\langle\phi_q\,|\,\phi_p{}^0\rangle$. Amplitudes in Figure 3 and 4 are plotted at ±0.05 a.u.

Acknowledgements

This work was support by the Deutsche Forschungsgemeinschaft (DFG, SPP 1415), the Friedrich-Ebert-Stiftung (G.T.), and the Studienstiftung des deutschen Volkes (Y.F.). We are indebted to R. Riedel for his help with X-ray crystallography and we thank Maximilian Fritz, Maximilian Jost, and Maximilian Biermeier for antecedent experimental studies.

Keywords: carbonyl homologues · crystal structures · DFT calculations · lead · rhodium clusters

How to cite: *Angew. Chem. Int. Ed.* **2015**, *54*, 11283–11288
Angew. Chem. **2015**, *127*, 11437–11442

[1] B. Meyer, J. J. Smith, K. Spitzer, *J. Chem. Phys.* **1970**, *53*, 3616–3620.
[2] For a recent review on CE^{16} (E^{16} = O…Te) see: a) Y. Mutoh, N. Kozono, K. Ikenaga, Y. Ishii, *Coord. Chem. Rev.* **2012**, *256*, 589–605, and references therein; for $E^{14}O$ (E^{14} = Sn, Pb) trapped by a benzannulated bisstannylene ligand see: b) A. V. Zabula, T. Pape, A. Hepp, F. M. Schappacher, U. C. Rodewald, R. Pöttgen, F. E. Hahn, *J. Am. Chem. Soc.* **2008**, *130*, 5648–5649; For contemporary $E^{14}E^{16}$ chemistry with non-metal-coordinated E^{14}–E^{16} units, see for example: c) G. He, O. Shynkaruk, M. W. Lui, E. Rivard, *Chem. Rev.* **2014**, *114*, 7815–7880; d) M. Bouška, L. Dostál, Z. Padělková, A. Lyčka, S. Herres-Pawlis, K. Jurkschat, R. Jambor, *Angew. Chem. Int. Ed.* **2012**, *51*, 3478–3482; *Angew. Chem.* **2012**, *124*, 3535–3540; e) S. S. Sen, S. Khan, P. P. Samuel, H. W. Roesky, *Chem. Sci.* **2012**, *3*, 659–682.
[3] K. P. Huber, G. Herzberg, *Molecular Structure and Molecular Spectra IV. Constants of Diatomic Molecules*, Van Nostrand Reinhold, New York, **1979**.
[4] a) J. Drowart, R. Colin, G. Exsteen, *Trans. Faraday Soc.* **1965**, *61*, 1376; b) C. Linton, H. P. Broida, *J. Mol. Spectrosc.* **1976**, *62*, 396–415.
[5] B. M. Giuliano, L. Bizzocchi, J.-U. Grabow, *J. Mol. Spectrosc.* **2008**, *251*, 261–267.
[6] B. M. Giuliano, L. Bizzocchi, R. Sanchez, P. Villanueva, V. Cortijo, M. E. Sanz, J.-U. Grabow, *J. Chem. Phys.* **2011**, *135*, 084303, and references therein.
[7] Z. J. Wu, *Chem. Phys. Lett.* **2003**, *370*, 39–43, and references therein.
[8] J.-M. Raulot, G. Baldinozzi, R. Seshadri, P. Cortona, *Solid State Sci.* **2002**, *4*, 467–474.
[9] D. Zagorac, K. Doll, J. C. Schön, M. Jansen, *Chem. Eur. J.* **2012**, *18*, 10929–10936.
[10] F. Demiray, S. Berber, *Phys. Scr.* **2013**, *88*, 015603–015603.
[11] P. Canepa, P. Ugliengo, M. Alfredsson, *J. Phys. Chem. C* **2012**, *116*, 21514–21522, and references therein.
[12] K. G. Dyall, *J. Chem. Phys.* **1993**, *98*, 2191–2197.
[13] S. Chattopadhyaya, A. Chattopadhyay, K. K. Das, *J. Phys. Chem. A* **2002**, *106*, 833–841.

[14] D. Shi, W. Xing, X. Zhang, J. Sun, Z. Zhu, Y. Liu, *Comput. Theor. Chem.* **2011**, *969*, 17 – 26, and references therein.
[15] S. Chattopadhyaya, K. K. Das, *Chem. Phys. Lett.* **2003**, *382*, 249 – 257, and references therein.
[16] A. F. Jalbout, X.-H. Li, H. Abou-Rachid, *Int. J. Quantum Chem.* **2007**, *107*, 522 – 539, and references therein.
[17] R. C. Oldenborg, C. R. Dickson, R. N. Zare, *J. Mol. Spectrosc.* **1975**, *58*, 283 – 300.
[18] E. S. Larsen, *Am. Mineral.* **1917**, *2*, 18 – 19.
[19] A. Walsh, G. W. Watson, *J. Solid State Chem.* **2005**, *178*, 1422 – 1428.
[20] G. Thiele, Z. You, S. Dehnen, *Inorg. Chem.* **2015**, *54*, 2491 – 2493.
[21] a) G. Thiele, PhD Thesis, Philipps-Universität Marburg, **2015**; b) G. Thiele, L. Vondung, S. Dehnen, *Z. Anorg. Allg. Chem.* **2015**, *641*, 247 – 252.
[22] J. A. Osborn, F. H. Jardine, J. F. Young, G. Wilkinson, *J. Chem. Soc. A* **1966**, 1711 – 1732.
[23] L. S. Ramsdell, *Am. Mineral.* **1925**, *10*, 281 – 304.
[24] a) A. N. Mariano, K. L. Chopra, *Appl. Phys. Lett.* **1967**, *10*, 282 – 284; b) T. K. Chattopadhyay, H. G. von Schnering, W. A. Grosshans, W. B. Holzapfel, *Physica B + C* **1986**, *139/140*, 356 – 360.
[25] M. Bremholm, Y. S. Hor, R. J. Cava, *Solid State Sci.* **2011**, *13*, 38 – 41.
[26] T. Balic-Zunic, E. Makovicky, *Can. Mineral.* **2007**, *45*, 437 – 443.
[27] C. W. Liu, T. S. Lobana, J.-L. Xiao, H.-Y. Liu, B.-J. Liaw, C.-M. Hung, Z. Lin, *Organometallics* **2005**, *24*, 4072 – 4078.
[28] P. A. W. Dean, J. J. Vittal, N. C. Payne, *Inorg. Chem.* **1984**, *23*, 4232.
[29] J. S. L. Yeo, J. J. Vittal, W. Henderson, T. S. A. Hor, *J. Chem. Soc. Dalton Trans.* **2002**, 328 – 336.
[30] Y.-J. Lu, J. A. Ibers, *Acta Crystallogr. Sect. C* **1991**, *47*, 1600.
[31] J. Lee, T. J. Emge, J. G. Brennan, *Inorg. Chem.* **1997**, *36*, 5064 – 5068.
[32] R. Hill, S. A. R. Knox, *J. Chem. Soc. Dalton Trans.* **1975**, 2622 – 2627.
[33] a) G. Thiele, T. Krüger, S. Dehnen, *Angew. Chem. Int. Ed.* **2014**, *53*, 4699 – 4703; *Angew. Chem.* **2014**, *126*, 4787 – 4791; b) benzene solvent isomer of **1**: $a = 18.0335(13)$, $b = 23.8399(16)$, $c = 25.7552(19)$ Å, $\beta = 106.032(2)°$, $V = 10642.0(13)$ Å^3; space group $P2_1$. Due to heavy disorder of solvent benzene and *en* molecules besides disorder of coordinating crown ether and *en* molecules, no dataset of sufficient quality for publication could be obtained so far.
[34] a) M. Björgvinsson, J. F. Sawyer, G. J. Schrobilgen, *Inorg. Chem.* **1987**, *26*, 741 – 749; b) H. Borrmann, J. Campbell, D. A. Dixon, H. P. A. Mercier, A. M. Pirani, G. J. Schrobilgen, *Inorg. Chem.* **1998**, *37*, 6656 – 6674.
[35] L. Jiang, Q. Xu, *Chem. Phys.* **2008**, *354*, 32 – 37.
[36] R. C. Fischer, P. P. Power, *Chem. Rev.* **2010**, *110*, 3877 – 3923.
[37] G. M. Sheldrick, SHELXL 2014. University of Göttingen, Germany, **2014**.
[38] OLEX2: a complete structure solution, refinement, and analysis program. O. V. Dolomanov, L. J. Bourhis, R. J. Gildea, J. A. K. Howard, H. Puschmann, *J. Appl. Crystallogr.* **2009**, *42*, 339 – 341.
[39] TURBOMOLE Version 6.6, TURBOMOLE GmbH 2014. TURBOMOLE is a development of University of Karlsruhe and Forschungszentrum Karlsruhe 1989 – 2007, TURBOMOLE GmbH since **2007**.
[40] F. Furche, R. Ahlrichs, C. Hättig, W. Klopper, M. Sierka, F. Weigend, *WIREs Comput. Mol. Sci.* **2014**, *4*, 91 – 100.
[41] F. Weigend, *Phys. Chem. Chem. Phys.* **2006**, *8*, 1057 – 1065.
[42] A. Klamt, G. Schüürmann, *J. Chem. Soc. Perkin Trans. 2* **1993**, 799 – 805.
[43] J. Tao, J. P. Perdew, V. N. Staroverov, G. E. Scuseria, *Phys. Rev. Lett.* **2003**, *91*, 146401.
[44] F. Weigend, A. Baldes, *J. Chem. Phys.* **2010**, *133*, 174102.
[45] K. A. Peterson, D. Figgen, M. Dolg, H. Stoll, *J. Chem. Phys.* **2007**, *126*, 124101.
[46] B. Metz, H. Stoll, M. Dolg, *J. Chem. Phys.* **2000**, *113*, 2563 – 2569.
[47] A. D. Becke, *Phys. Rev. A* **1988**, *38*, 3098 – 3100.
[48] J. P. Perdew, *Phys. Rev. B* **1986**, *33*, 8822 – 8824.
[49] M. v. Hopffgarten, G. Frenking, *WIREs Comput. Mol. Sci.* **2012**, *2*, 43 – 62.

Received: May 28, 2015
Revised: June 26, 2015
Published online: July 31, 2015

